JACS
JOURNAL OF THE AMERICAN CHEMICAL SOCIETY

Communication

pubs.acs.org/JACS

Specific Detection of Integrin $\alpha_v\beta_3$ by Light-Up Bioprobe with Aggregation-Induced Emission Characteristics

Haibin Shi,[†] Jianzhao Liu,[‡] Junlong Geng,[†] Ben Zhong Tang,*[,‡,§] and Bin Liu*[,†,§]

[†]Department of Chemical and Biomolecular Engineering, 4 Engineering Drive 4, National University of Singapore, 117576, Singapore

[‡]Department of Chemistry, Institute for Advanced Study, State Key Laboratory of Molecular Neuroscience, Institute of Molecular Functional Materials, and Division of Biomedical Engineering, The Hong Kong University of Science and Technology, Clear Water Bay, Kowloon, Hong Kong, China

[§]Institute of Materials Research and Engineering, 3 Research Link, 117602, Singapore

Supporting Information

ABSTRACT: Specific bioprobes with fluorescence turn-on response are highly desirable for high contrast biosensing and imaging. In this work, we developed a new generation bioprobe by integrating tetraphenylsilole, a fluorogenic unit with aggregation-induced emission (AIE) characteristic, with cyclic arginine−glycine−aspartic acid tripeptide (cRGD), a targeting ligand to integrin $\alpha_v\beta_3$ receptor. Emission of the AIE probe is switched *on* upon its specific binding to integrin $\alpha_v\beta_3$, which allows quantitative detection of integrin $\alpha_v\beta_3$ in solution and real-time imaging of the binding process between cRGD and integrin $\alpha_v\beta_3$ on cell membrane. The probe can be used for tracking integrin $\alpha_v\beta_3$ and for identifying integrin $\alpha_v\beta_3$-positive cancer cells.

Researchers are in enthusiastic pursuit of fluorescent probes for targeted bioimaging of tumor cells owing to their potential applications in cancer diagnostics and clinical surgery.[1] High selectivity and sensitivity are the primary requirements for a fluorescent probe to be practically useful. The selectivity is largely determined by the affinity between specific ligands and biomarkers, while the sensitivity is usually dependent on the fluorescence contrast before and after probe binding to cancer cells. As "conventional" fluorescent bioprobes are normally emissive in the physiological buffer, it is rather difficult to discriminate the nonspecific probe emission in the aqueous medium (background) from that of the probe localized at the target of interest. This necessitates multiple washing steps in vitro or natural clearance in vivo to minimize the background interference and to increase the signal-to-noise ratio, which is incompatible with continuous sensing or monitoring of biological processes and events.[2]

Water solubility is a prerequisite for bioprobes, which is typically achieved by attaching hydrophilic groups to organic fluorophores. This generally produces amphiphilic molecules, which tend to aggregate via $\pi-\pi$ stacking or upon interacting with bioanalytes. The aggregate formation often quenches the fluorescence to a great extent,[3] leading to a large reduction in the probe sensitivity. To tackle this issue, it is highly desirable to develop fluorescence-silent bioprobes that are free of the aggregation-caused quenching (ACQ) effect and show light-up response to specific analytes.

We have observed a novel photophysical phenomenon of aggregation-induced emission (AIE), which is opposite to the ACQ effect discussed above. In an AIE system, a nonemissive fluorogen in a dilute solution is induced to emit efficiently by aggregate formation.[4,5] A large number of experimental and theoretical studies have revealed that the restriction of intramolecular rotations (RIR) in the aggregates is the main cause for the AIE process. Taking advantage of the AIE effect, a variety of fluorogens with emission efficiencies of up to unity in the aggregate state have been developed for applications as chemical sensors, biological probes, and active layers in light-emitting diodes.[4−11]

Water-soluble ionic AIE fluorogens have been found to show fluorescence turn-on responses to biomolecules, such as DNA, RNA, proteins, and sugars, through activation of the RIR process by the involved probe−analyte interactions.[6−9] As the interactive forces between the AIE fluorogens and biomolecules have been mainly electrostatic and hydrophobic in nature, poor or no selectivity to bioanalytes has been observed. So far, the only successful example of AIE probe for specific analyte binding is the carbohydrate-bearing tetraphenylethene (TPE), which has enabled the study of carbohydrate−lectin interaction and protein displacement in aqueous media.[10,11] The absorption of TPE in the biologically harmful UV region (250−350 nm), however, has hampered the AIE probe from finding bioimaging applications.

The fluorescence turn-on characteristics of AIE fluorogens have motivated us to develop specific probes for bioimaging. In this project, we worked on the design and synthesis of an AIE probe for specific biomarker protein detection. Integrin $\alpha_v\beta_3$ was chosen as a model protein target, as it plays a critical role in regulating tumor growth and metastasis.[12] It is overexpressed on tumor cells of different origins, with the levels of expressions correlating well with the aggressiveness of the diseases.[12a,13] As a receptor for the extracellular matrix protein with exposed arginine−glycine−aspartic acid (RGD) sequence, integrin $\alpha_v\beta_3$ is a unique molecular target for early detection and treatment of rapidly growing solid tumors.[14] Considering the high affinity and specificity of cyclic RGD tripeptide (cRGD) to integrin $\alpha_v\beta_3$, we integrated two cRGD units with one tetraphenylsilole

Received: March 19, 2012
Published: May 29, 2012

dx.doi.org/10.1021/ja302369e | *J. Am. Chem. Soc.* 2012, 134, 9569−9572

(TPS) unit, a typical AIE fluorogen,[4d] and succeeded in creating the first example of AIE bioprobe (TPS-2cRGD) for specific integrin $\alpha_v\beta_3$ sensing and imaging. As compared to the widely used radioactive bioprobes,[15,16] our fluorescence light-up probe provides a safer, simpler, and more economic solution to protein biomarker detection.

The TPS-2cRGD conjugate was synthesized by a copper-catalyzed "click" reaction of a bisazido (BA)-functionalized TPS (BATPS) with an ethylyne (E)-bearing cRGD (E-cRGD; GL Biochem Ltd.) in a DMSO/water mixture[17] (Scheme 1).

Scheme 1. "Click" Synthesis of TPS-2cRGD Probe

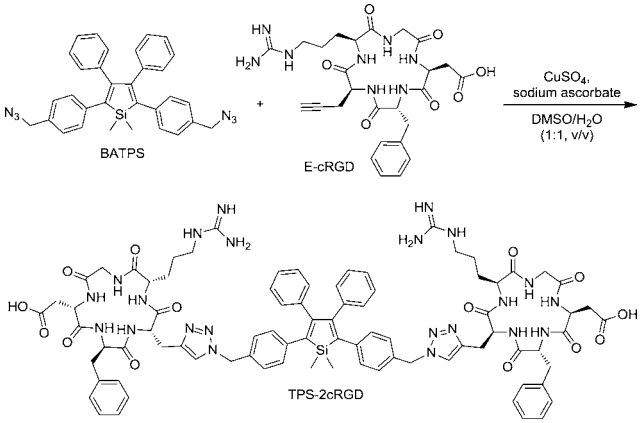

BATPS was prepared in 57% yield by the synthetic route shown in Scheme S1 in the Supporting Information (SI). Its MS and NMR spectra are depicted in SI Figures S1 and S2. Its click reaction in the presence of $CuSO_4$/sodium ascorbate afforded TPS-2cRGD in 80% yield. The purity and identity of the click product were verified by analytical HPLC, HR–MS, ^{1}H NMR, and FT-IR (SI Figures S3–S5).

BATPS and TPS-2cRGD show similar absorption spectral profiles, with absorption edges of up to 450 nm (SI Figure S6A), which allows them to be excited with a 405 nm laser. It is known that an AIE fluorogen is nonemissive in a good solvent but emits intensely when aggregated in a poor solvent.[4] As shown in Figure 1A, BATPS emits strong fluorescence as nanoaggregates in a mixture of DMSO/water (1:199 by vol),[18] whereas TPS-2cRGD does not fluoresce in the same medium, due to its good solubility in water. The aggregate formation of the former and the molecular dissolution of the latter were confirmed by laser light scattering (LLS) measurements. In the aqueous mixture, the hydrophobic BATPS molecules cluster into aggregates with an average diameter of 103 nm (SI Figure S6B). No LLS signals, however, could be collected from the solution of the hydrophilic TPS-2cRGD.

As biosensing is often conducted in an aqueous buffer, it is important to study the effect of ionic strength on the emission behavior of the probe. The experiments were performed with addition of sodium chloride into an aqueous solution of TPS-2cRGD (10 μM). Little change in the photoluminescence (PL) spectrum of the probe is observed when the concentration of NaCl is increased from 0 to 960 mM (SI Figure S7). Clearly, ionic strength does not affect the fluorescence property of TPS-2cRGD. Its PL spectrum does not change either in the presence of the Dulbecco's Modified Eagle Medium, which contains amino acids, salts, glucose and vitamins. The probe maintains an "off" state in the complex environment and thus has great

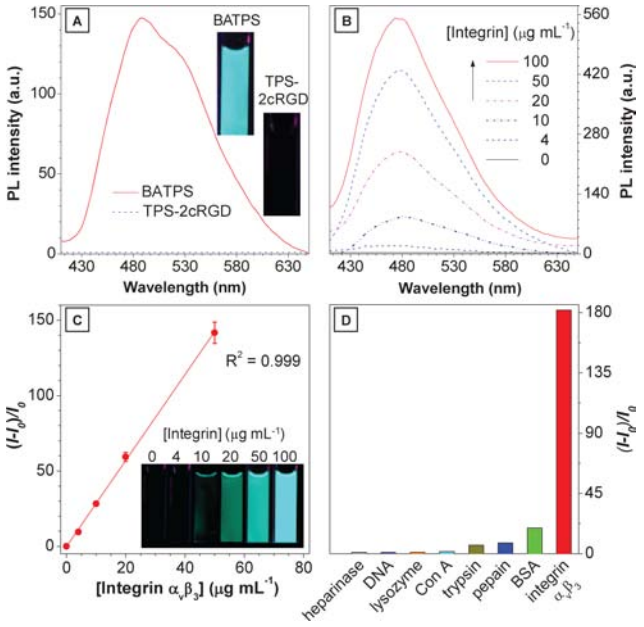

Figure 1. (A) PL spectra of BATPS and TPS-2cRGD in a mixture of DMSO/water (1:199 v/v). Inset: Their photographs taken under illumination of a UV lamp. (B) PL spectra of TPS-2cRGD in the presence of different amounts of integrin $\alpha_v\beta_3$. (C) Plot of $(I - I_0)/I_0$ versus concentration of integrin $\alpha_v\beta_3$ in PBS buffer. I and I_0 are the PL intensities of TPS-2cRGD in the presence and absence of integrin $\alpha_v\beta_3$, respectively. Inset: Photographs taken under UV illumination. (D) Plot of $(I - I_0)/I_0$ versus different proteins and DNA, where I and I_0 are the PL intensities at analyte concentrations of 100 and 0 μg mL^{-1}, respectively. [BATPS] = [TPS-2cRGD] = 10 μM; λ_{ex} = 356 nm.

potential to serve as a specific light-up probe with minimum background interference.

Our assay design rationale is illustrated in Scheme 2. As TPS-2cRGD is miscible with water, the excited states of its isolated

Scheme 2. Discrimination of (A) Integrin $\alpha_v\beta_3$ from (B) Other Proteins via Specific cRGD–Integrin Interaction

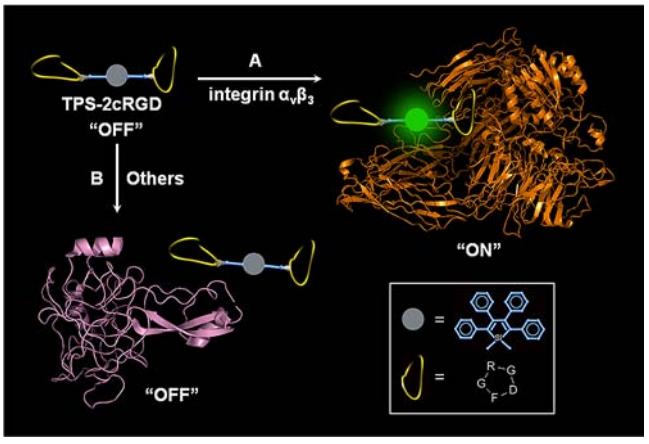

molecules in a dilute aqueous solution are readily annihilated nonradiatively by the free intramolecular rotations of its multiple phenyl rotors (cf., Figure 1A).[4d] Addition of a protein into the aqueous solution may result in two scenarios. Scenario A refers to the addition of a probe-specific protein, for example, integrin $\alpha_v\beta_3$. The specific binding between TPS-2cRGD and integrin $\alpha_v\beta_3$ will dramatically restrict the intramolecular

dx.doi.org/10.1021/ja302369e | J. Am. Chem. Soc. 2012, 134, 9569–9572

rotations of the aromatic rotors, leading to fluorescence light-up of the probe, according to the RIR mechanism of the AIE process. When a protein has no specific interaction with TPS-2cRGD, however, the solution should remain in the dark state (scenario B).

To test our hypothesis, titration experiments were carried out by adding different amounts of human integrin $\alpha_v\beta_3$ into a TPS-2cRGD solution (10 μM) in the PBS buffer containing 137 mM NaCl, 2.7 mM KCl, 10 mM Na_2HPO_4, and 2 mM KH_2PO_4 at pH 7.4. Figure 1B shows the variation in the PL spectrum of TPS-2cRGD with the concentration of the added integrin $\alpha_v\beta_3$. The corresponding photographs are shown in the inset of Figure 1C. With increasing concentration of integrin $\alpha_v\beta_3$, the PL spectrum of TPS-2cRGD is progressively intensified. In comparison to its emission in the buffer solution, a 182-fold PL enhancement is observed when the AIE probe is incubated with 100 μg mL^{-1} of integrin $\alpha_v\beta_3$.

As each integrin $\alpha_v\beta_3$ has only one binding site for cRGD in between the α and β domains,[16] each probe can only bind to one integrin $\alpha_v\beta_3$. As such, the PL enhancement is caused by the RIR process of the phenyl rotors in the silole core, due to the formation of complex between TPS-2cRGD and integrin $\alpha_v\beta_3$. Plot of the net changes in the PL intensity against the protein concentration below 50 μg mL^{-1} gives a perfect linear line (Figure 1C), suggesting the possibility of using the TPS-2cRGD probe for integrin quantification. The detection limit for integrin $\alpha_v\beta_3$ is estimated to be 0.5 μg mL^{-1}.

To investigate the selectivity of the probe, TPS-2cRGD was treated under identical conditions with DNA and several proteins other than human integrin $\alpha_v\beta_3$ with varying isoelectric points (pI), such as heparinase (pI = 7.9), lysozyme (pI = 11.0), concanavalin A (Con A, pI = 8.4), trypsin (pI = 10.1), papain (pI = 8.7), and BSA (pI = 4.9). As can be seen from Figure 1D, integrin $\alpha_v\beta_3$ displays ~10- to 182-fold larger changes in $(I - I_0)/I_0$ than the other six proteins. This substantiates that TPS-2cRGD is indeed a specific probe for human integrin $\alpha_v\beta_3$.

To explore the possibility of using TPS-2cRGD as a specific bioprobe for in vitro integrin detection, its receptor-mediated binding to integrin $\alpha_v\beta_3$ was examined in mammalian cells. Colon cancer cell HT-29 with overexpressed integrin $\alpha_v\beta_3$ on cellular membrane was chosen as integrin-positive cancer cell, while breast cancer cell MCF-7 with a low level of integrin $\alpha_v\beta_3$ expression was used as a negative control.[19] Figure 2 shows confocal laser scanning microscopy (CLSM) images of HT-29 and MCF-7 live cells after incubation with TPS-2cRGD. A commercial membrane tracker was used to visualize the location of the cell membranes (Figure 2B,E,H). The images were taken under excitation at 405 nm with a 505−525 nm band-pass filter for the probe and at 543 nm with a 575−635 nm band-pass filter for the membrane tracker. No autofluorescence signals from the cells were detected under these experimental conditions.

As can be seen from Figure 2A, MCF-7 breast cancer cells afford very weak fluorescence. In sharp contrast, under the identical experimental conditions, obvious fluorescence signals are collected from HT-29 colon cancer cells (Figure 2D). The signals are greatly reduced when the cells have been pretreated with free cRGD peptide (Figure 2G), manifesting that the fluorescence is originated from specific binding between TPS-2cRGD and integrin $\alpha_v\beta_3$. Furthermore, the excellent overlap between the fluorescence images of the probe and the membrane tracker corroborates that the specific binding occurs

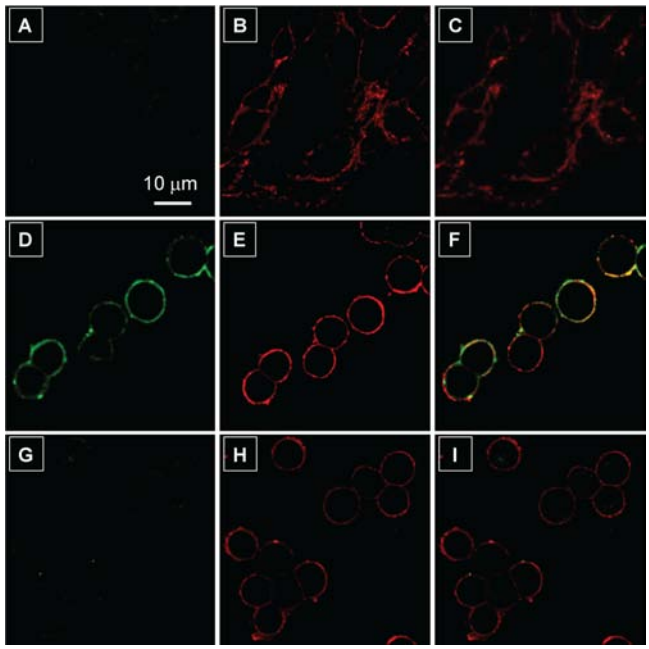

Figure 2. CLSM images of live cells after incubation with 2 μM TPS-2cRGD in the absence and presence of a membrane tracker (62.5 ng mL^{-1}) for 30 min at 4 °C. Fluorescence images of (A−C) MCF-7 and (D−F) HT-29 cells stained by (A, D) TPS-2cRGD and (B, E) membrane tracker, with (C, F) their overlay images. Fluorescence images of HT-29 cells pretreated with 10 μM cRGD followed by staining by (G) TPS-2cRGD and (H) membrane tracker, with (I) their overlay image. The images were taken under excitations at (A, D, G) 405 nm and (B, E, H) 543 nm using optical filters with band passes of (A, D, G) 505−525 nm and (B, E, H) 575−635 nm at 5% laser power. All images share the same scale bar (10 μm).

on the cellular membrane (Figure 2F). The specific interaction between TPS-2cRGD and integrin $\alpha_v\beta_3$ enables unambiguous discrimination between integrin $\alpha_v\beta_3$-negative and -positive cancer cells (cf., Figure 2A,D).

Norman et al. have recently found that at 22 and 37 °C, integrin $\alpha_v\beta_3$ can be internalized into live cells.[20] To study the TPS-2cRGD/integrin interaction and monitor the integrin $\alpha_v\beta_3$ internalization, real-time imaging was taken with HT-29 live cells at room temperature, instead of at 4 °C (cf., Figure 2). The dark background in each of the images shown in Figure 3 indicates that the bioprobe is nonfluorescent in the cell growth

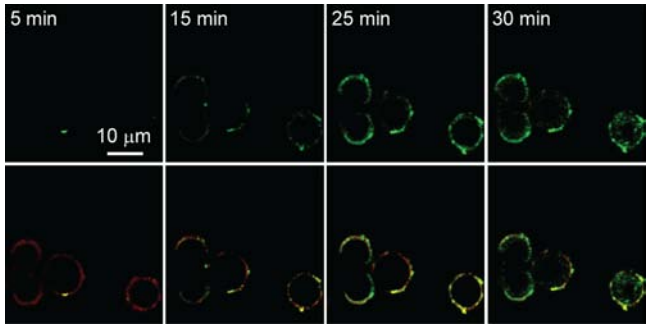

Figure 3. Real-time fluorescence images showing TPS-2cRGD interactions with HT-29 cells at room temperature (top panel). Overlay images of cells stained with TPS-2cRGD and membrane tracker (bottom panel). All images have the same scale bar (10 μm). See the movie in the SI for the dynamic imaging process.

dx.doi.org/10.1021/ja302369e | J. Am. Chem. Soc. 2012, 134, 9569−9572

media. In the first 25 min, as incubation time elapses, the fluorescence intensity increases with the progress in the probe binding to integrin $\alpha_v\beta_3$. The green fluorescence from the probe overlaps well with the red fluorescence from the membrane tracker. Clearly, during this period of time, most of the bound probes are localized on the cell membranes. Longer incubation time (>25 min) results in gradual internalization of the probe. In addition, HPLC analysis reveals that the probe has good stability in the cellular environment for 2 h (SI Figure S8). Collectively, these results show that TPS-2cRGD not only can be used for the detection of integrin $\alpha_v\beta_3$-positive cancer cells, but also has the potential to become a powerful bioprobe for studying interaction with integrin $\alpha_v\beta_3$ and tracing the integrin $\alpha_v\beta_3$ internalization in a real-time manner.

Cytotoxicity of the fluorescent probe was evaluated by the widely used MTT assay. As shown in SI Figure S9, after being incubated with TPS-2cRGD at concentrations of 2, 5, and 10 μM for 12, 24, and 48 h, the HT-29 cells remain ~100% metabolically viable under the testing conditions, indicative of excellent cyto-compatibility of the fluorescent probe.

In summary, a cRGD-conjugated probe has been developed in this work. Thanks to its novel AIE nature, the probe is nonfluorescent in the aqueous buffer but becomes emissive when bound to integrin $\alpha_v\beta_3$, which enables integrin detection with little background interference. The binding affinity of TPS-2cRGD to HT-29 over MCF-7 demonstrates its potential as a specific probe for discriminating integrin $\alpha_v\beta_3$-positive cancer cells from integrin $\alpha_v\beta_3$-negative cancer cells. To the best of our knowledge, this is the first fluorescence light-up probe for the detection of endogenous human integrin receptor in live cells. It also represents the first AIE bioprobe for specific real-time biomarker imaging, which opens new avenues for continuous monitoring of biological events. Our AIE probe strategy can be generalized to perform various tasks by simply changing peptide into other biorecognition units, such as antibodies, aptamers, and ligands. Further tuning the emission spectrum of the AIE fluorogen to red and near-IR region will facilitate the development of specific bioprobes for in vivo tumor diagnosis.

■ ASSOCIATED CONTENT

Supporting Information

Detailed experimental procedures; structural characterization data of BATPS and TPS-2cRGD; particle size distribution of BATPS, absorption spectra of BATPS and TPS-2cRGD, and PL spectra of TPS-2cRGD with varying concentrations of NaCl in DMSO/water and in cell culture medium; stability and cytotoxicity data of TPS-2cRGD; movie showing the dynamic process of cell imaging. This material is available free of charge via the Internet at http://pubs.acs.org.

■ AUTHOR INFORMATION

Corresponding Author

cheliub@nus.edu.sg; tangbenz@ust.hk

Notes

The authors declare no competing financial interest.

■ ACKNOWLEDGMENTS

We thank the Singapore National Research Foundation (R-279-000-323-281), the Research Grants Council of Hong Kong (HKUST2/CRF/10 and N_HKUST620/11), and the Institute of Materials Research and Engineering of Singapore (IMRE/11-1C0213).

■ REFERENCES

(1) van Dam, G. M.; et al. *Nat. Med.* **2011**, *17*, 1315−1319.
(2) Kobayashi, H.; Ogawa, M.; Alford, R.; Choyke, P. L.; Urano, Y. *Chem. Rev.* **2010**, *110*, 2620−2640.
(3) Birks, J. B. *Photophysics of Aromatic Molecules*; Wiley: London, 1970.
(4) (a) Luo, J.; et al. *Chem. Commun.* **2001**, 1740−1741. (b) Hong, Y. N.; Lam, J. W. Y.; Tang, B. Z. *Chem. Commun.* **2009**, 4332−4353. (c) Yu, Y.; Feng, C.; Hong, Y. N.; Liu, J. Z.; Chen, S. J.; Ng, K. M.; Luo, K. Q.; Tang, B. Z. *Adv. Mater.* **2011**, *23*, 3298−3302. (d) Hong, Y.; Lam, J. W. Y.; Tang, B. Z. *Chem. Soc. Rev.* **2011**, *40*, 5361−5388. (e) Qin, W.; Ding, D.; Liu, J. Z.; Wang, Z. Y.; Hu, Y.; Liu, B.; Tang, B. Z. *Adv. Funct. Mater.* **2012**, *22*, 771−779.
(5) Chen, J. W.; Law, C. C. W.; Lam, J. W. Y.; Dong, Y. P.; Lo, S. M. F.; Williams, I. D.; Zhu, D. B.; Tang, B. Z. *Chem. Mater.* **2003**, *15*, 1535−1546.
(6) Hatano, K.; Saeki, H.; Yokota, H.; Aizawa, H.; Koyama, T.; Matsuoka, K.; Terunuma, D. *Tetrahedron Lett.* **2009**, *50*, 5816−5819.
(7) Dong, Y. Q.; Lam, J. W. Y.; Qin, A.; Li, Z.; Liu, J. Z.; Sun, J. Z.; Dong, Y. P.; Tang, B. Z. *Chem. Phys. Lett.* **2007**, *446*, 124−126.
(8) Wang, M.; Zhang, D. Q.; Zhang, G. X.; Zhu, D. B. *Chem. Commun.* **2008**, 4469−4471.
(9) (a) Tong, H.; Hong, Y. N.; Dong, Y. Q.; Haußler, M.; Lam, J. W. Y.; Li, Z.; Guo, Z. F.; Guo, Z. H.; Tang, B. Z. *Chem. Commun.* **2006**, 3705−3707. (b) Liu, Y.; Deng, C. M.; Tang, L.; Qin, A. J.; Hu, R. R.; Sun, J. Z.; Tang, B. Z. *J. Am. Chem. Soc.* **2011**, *133*, 660−663. (c) Hong, Y.; et al. *J. Am. Chem. Soc.* **2012**, *134*, 1680−1689. (d) Wang, M.; Zhang, G. X.; Zhang, D. Q.; Zhu, D. B.; Tang, B. Z. *J. Mater. Chem.* **2010**, *20*, 1858−1867.
(10) (a) Sanji, T.; Shiraishi, K.; Nakamura, M.; Tanaka, M. *Chem. Asian J.* **2010**, *5*, 817−824. (b) Shiraishi, K.; Sanji, T.; Tanaka, M. *Tetrahedron Lett.* **2010**, *51*, 6331−6333.
(11) Hu, X. M.; Chen, Q.; Wang, J. X.; Cheng, Q. Y.; Yan, C. G.; Cao, J.; He, Y. J.; Han, B. H. *Chem. Asian J.* **2011**, *6*, 2376−2381.
(12) (a) Nisato, R. E.; Tille, J. C.; Jonczyk, A.; Goodman, S. L.; Pepper, M. S. *Angiogenesis* **2003**, *6*, 105−119. (b) Hodivala-Dilke, K. M.; Reynolds, A. R.; Reynolds, L. E. *Cell Tissue Res.* **2003**, *314*, 131−144. (c) Cairns, R. A.; Khokha, R.; Hill, R. P. *Curr. Mol. Med.* **2003**, *3*, 659−571. (d) Felding-Habermann, B. *Clin. Exp. Metastasis* **2003**, *20*, 203−213.
(13) Gasparini, G.; Brooks, P. C.; Biganzoli, E.; Vermeulen, P. B.; Bonoldi, E.; Dirix, L. Y.; Ranieri, G.; Miceli, R.; Cheres, D. A. *Clin. Cancer Res.* **1998**, *4*, 2625−2634.
(14) (a) Chen, X. Y.; Conti, P. S.; Moats, R. A. *Cancer Res.* **2004**, *64*, 8009−8014. (b) Themelis, G.; Harlaar, N. J.; Kelder, W.; Bart, J.; Sarantopoulos, A.; van Dam, G. M.; Ntziachristos, V. *Ann. Surg. Oncol.* **2011**, *18*, 3506−3513.
(15) Zitzmann, S.; Ehemann, V.; Schwab, M. *Cancer Res.* **2002**, *62*, 5139−5143.
(16) Liu, S. *Bioconjugate Chem.* **2009**, *20*, 2199−2213.
(17) (a) Kolb, H. C.; Sharpless, K. B. *Drug Discovery Today* **2003**, *8*, 1128−1137. (b) Meldal, M.; Tornøe, C. W. *Chem. Rev.* **2008**, *108*, 2952−3015.
(18) (a) Liu, J.; Lam, J. W. Y.; Tang, B. Z. *J. Inorg. Organomet. Polym. Mater.* **2009**, *19*, 249−285. (b) Liu, J.; Lam, J. W. Y.; Tang, B. Z. *Chem. Rev.* **2009**, *109*, 5799−5867.
(19) Taherian, A.; Li, X. L.; Liu, Y. Q.; Haas, T. A. *BMC Cancer* **2011**, *11*, 293−308.
(20) Roberts, M.; Barry, S.; Woods, A.; van der Slujis, P.; Norman, P. *Curr. Biol.* **2001**, *11*, 1392−1402.